Combined RS-EPI and SAP-EPI for High Resolution Diffusion-Weighted Imaging

Murat Aksoy[1], Samantha J Holdsworth[1], Rafael O'Halloran[1], and Roland Bammer[1]
[1]*Center for Quantitative Neuroimaging, Department of Radiology, Stanford University, Stanford, CA, United States*

Introduction: 'Short-Axis readout Propeller EPI' (SAP-EPI) [1] and 'Readout-Segmented EPI' (RS-EPI) [2,3] have been proposed for use in high-resolution diffusion-weighted (DW) imaging (Fig. 1). SAP-EPI and RS-EPI share common characteristics, in that *k*-space is traversed by several EPI 'segments' (referred to as blades (SAP-EPI) or blinds (RS-EPI)) in order to reduce the distortion that typically hampers EPI images. One disadvantage of RS-EPI is that it requires an additional navigator blind in order to phase-correct off-center readout blinds, and is typically discarded (thus reducing the scan time efficiency). In this work, we propose the use of RS-EPI with rotating navigator (a.k.a. SAP-EPI) blades and present preliminary data. For this combined RS-EPI and SAP-EPI (RS-SAP EPI) sequence, each blade can be rotated and used to phase correct the RS-EPI blinds, while the combination of the SAP-EPI 'navigator' blades can form an additional image with complementary DW contrast information.

Methods: RS-SAP EPI diffusion-weighted images were acquired on a human volunteer using a 3T whole-body MRI unit (GE Discovery MR750) with a high-performance gradient system (50 mT/m, SLR=200 mT/m/s), and an 8-channel head coil. The scan parameters were: 256×256 with a blade/blind width = 32, FOV = 24 cm, #blades/#blinds = 9, slice thickness = 5 mm, TR = 10 s; TE_{RS}/TE_{SAP}=75ms/160ms; partial Fourier with 52 overscans, Stejskal-Tanner diffusion preparation, one b = 0, and three b = 1000 s/mm^2 with x,y,z diffusion encoding (Fig. 1). The SAP-EPI portion of the RS-SAP acquisition was used for two purposes: (1) correction of the phase errors in both the RS-EPI and SAP-EPI acquisition, and (2) reconstruction of a second high resolution SAP-EPI diffusion-weighted image with a longer TE (thus higher T2-weighting). A separate RS-EPI diffusion-weighted scan with identical imaging parameters was acquired for comparison. Phase correction of the data was performed using a triangular-windowing approach [5] with a k-space radius of 32 points.

Results: Fig. 2 compares the separately acquired standard RS-EPI diffusion-weighted images with the RS-SAP EPI approach. It can be seen that the SAP-EPI navigator successfully corrected for the phase errors in the RS-EPI acquisition and is of similar quality to that of the separately required RS-EPI acquisition. The SAP-EPI image itself has comparatively reduced SNR and greater extent of image blurring, but may offer additional information as shown by the increased gray/white matter contrast.

Discussion & Conclusion: This study demonstrates that high resolution RS-EPI images can be acquired with the use of a rotating navigator blind, while the navigator blinds themselves can be used to form a SAP-EPI diffusion-weighted image. The additional SAP-EPI diffusion-weighted image acquisition results in no penalty in scan time as compared to standard RS-EPI. In the RS-SAP DWI acquisition, while the RS-EPI images are higher SNR and are sharper due the unidirectional distortion of the blinds, the SAP-EPI provides greater T2 weighting - which could be useful for increased sensitivity of lesions in a clinical setting. Further improvements to RS-SAP EPI are possible through use of parallel imaging and retrospective distortion correction [4].

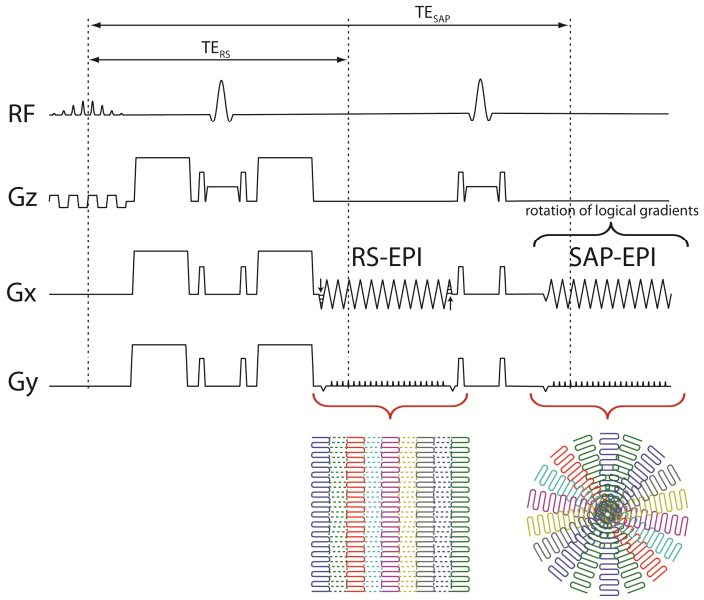

Figure 1 – Combined readout-segmented and short axis propeller EPI (RS-SAP EPI) sequence. The RS-EPI acquisition gives a high resolution DW image, and the SAP-EPI acquisition is used to correct phase errors of both acquisitions, and to get second high resolution diffusion weighted image at a longer .

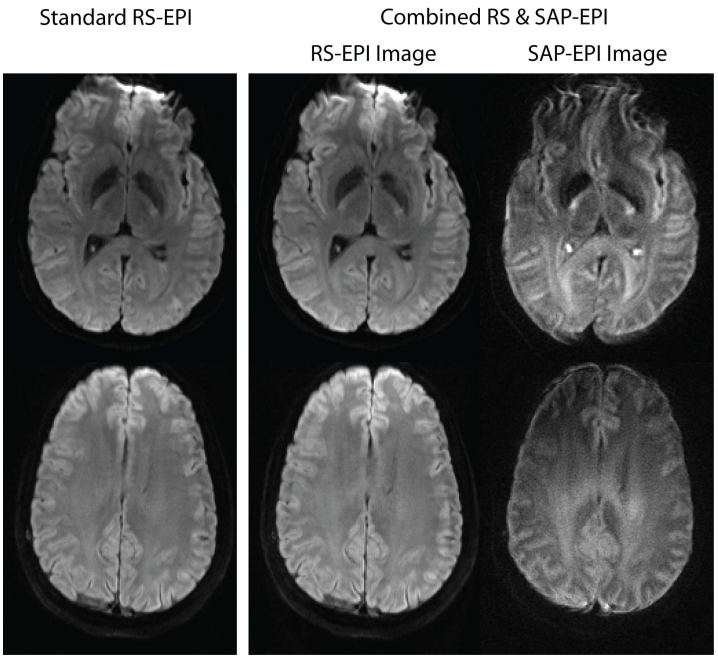

Figure 2 – Isotropic DW images for standard RS-EPI (left column) and combined RS (middle column) and SAP –EPI (right column).

References: - [1] Skare S. MRM 2006, 55:1298-1307. [2] Porter D, MRM, 62:468, 2009. [3] Holdsworth, S. MRM, 62:1629, 2009. [4] Skare, S. ISMRM, 2010:192. [5] Pipe J, MRM, 1999; 42(5):963-969**Acknowledgements:** This work was supported in part by the NIH (1R01EB008706, 1R01EB008706S1, 5R01EB002711, 1R01EB006526, 1R21EB006860), the Center of Advanced MR Technology at Stanford (P41RR09784), Lucas Foundation, and Oak Foundation.